Vol. 726: 17–30, 2024
https://doi.org/10.3354/meps14474

MARINE ECOLOGY PROGRESS SERIES
Mar Ecol Prog Ser

Published January 11

Assessing inorganic nitrogen transport in marine phytoplankton assemblages through the ^{15}N-tracer technique and metatranscriptomics

Chi-Yu Shih[1,2], Kai-Zhe Chang[1,3], Pei-Ling Wang[4], Jeng Chang[3,5,6], Lee-Kuo Kang[1,2,3,6,*]

[1]Bachelor Degree Program in Marine Biotechnology, National Taiwan Ocean University, Keelung 20224, Taiwan, ROC
[2]Taiwan Ocean Genome Center, National Taiwan Ocean University, Keelung 20224, Taiwan, ROC
[3]Institute of Marine Environment and Ecology, National Taiwan Ocean University, Keelung 20224, Taiwan, ROC
[4]Institute of Oceanography, National Taiwan University, Taipei 10617, Taiwan, ROC
[5]Institute of Marine Biology, National Taiwan Ocean University, Keelung 20224, Taiwan, ROC
[6]Center of Excellence for the Oceans, National Taiwan Ocean University, Keelung 20224, Taiwan, ROC

ABSTRACT: The availability of inorganic nitrogen is considered one of the limiting factors for primary production in the ocean. However, different phytoplankton possess unique strategies to take up and assimilate nitrate and ammonium to cope with environmental changes. To investigate the nitrogen uptake characteristics of different size-fractionated phytoplankton in natural assemblages, 3 research cruises were conducted in the southern East China Sea in 2018 and 2019. The nitrogen uptake characteristics of 2 size-fractionated natural assemblages, microphytoplankton (20–200 µm) and pico-nanophytoplankton (<20 µm), were measured using the ^{15}N-tracer technique. At most of the stations, significantly higher potential maximum uptake rates of ammonium than of nitrate were detected in the pico-nanophytoplankton, indicating that small phytoplankton possess a relatively superior capacity to take up ammonium. By contrast, comparing the potential maximum uptake rate for nitrate between microphytoplankton and pico-nanophytoplankton showed that microphytoplankton exhibit a higher capacity for nitrate uptake as a nitrogen source compared to pico-nanophytoplankton. However, repressed uptake rates of ammonium and nitrate in microphytoplankton were sometimes found at the coastal station even when ambient nitrate concentrations remained high. Metatranscriptomic analysis of nitrogen transporter genes in microphytoplankton suggests that most diatoms utilize regenerated ammonium before nitrate to maintain their populations at the end of blooms. Metatranscriptomic approaches identify the transcriptional responses of dominant diatoms to explain how diatoms regulate their nitrogen transporter genes to cope with environmental changes in natural assemblages.

KEY WORDS: Phytoplankton · Nitrogen uptake · Nitrate · Ammonium · Nitrogen transporter genes · Metatranscriptome · Southern East China Sea

1. INTRODUCTION

Nitrogen is often considered the major limiting factor to the growth of phytoplankton in the marine environment (Downing et al. 1999). The major bioavailable inorganic nitrogen forms for phytoplankton are nitrate and ammonium. Past studies have shown that phytoplankton of different sizes have their own uptake preferences for nitrate and ammonium (Litchman et al. 2007, Edwards et al. 2012, Marañón et al.

*Corresponding author: lkkang@mail.ntou.edu.tw

2013, Glibert et al. 2016). For example, large phytoplankton, such as diatoms, are nitrate specialists, while small phytoplankton, such as cyanobacteria and small dinoflagellates, are successful competitors for ammonium (Lomas & Glibert 2000, Glibert et al. 2016 and references therein). Therefore, when the proportion of nitrate and ammonium supply changes in a natural system, the major primary productivity contributors and dominant functional groups in a phytoplankton community will shift accordingly.

In the past, investigations of nitrogen uptake kinetics in natural assemblages have provided information that clarified the relationship between phytoplankton community succession and ambient nitrogen supply (MacIsaac & Dugdale 1969, Glibert & McCarthy 1984, Kanda et al. 1985, Collos et al. 2005, Li et al. 2010, Xu et al. 2012). In laboratory experiments, the Michaelis-Menten equation is commonly applied to estimate uptake parameters, including the maximum uptake rate and half-saturation constant, to understand the nitrogen uptake kinetics of individual phytoplankton (Eppley et al. 1969, Falkowski 1975). However, laboratory experiments have indicated that nitrogen uptake parameters vary with physiological states, including nutritional conditions, feedback inhibition of ammonium, and intracellular nitrogen pools (Dortch 1982, Harrison et al. 1989, McGlathery et al. 1996, Flynn et al. 1997). In comparison to laboratory conditions, the natural environmental conditions of field investigations are much more complex, and *in situ* nitrogen uptake kinetics could be affected by the interactions among the multiple forms of nitrogen (e.g. Dortch 1990) and the competition among phytoplankton groups (e.g. Glibert et al. 2016). Therefore, investigations of *in situ* nitrogen uptake kinetics from natural assemblages in addition to their corresponding physiological states provide us with more information to explain how phytoplankton regulate their uptake systems to cope with environmental changes in the ocean.

Recently, molecular studies of phytoplankton gene expression have provided another avenue for understanding the regulation of the nitrogen uptake system and physiological states in response to various nitrogen conditions. Regarding nitrogen uptake, inorganic nitrogen transporters such as nitrate transporters (NRT2 family) and ammonium transporters (AMT1 family) are considered to play crucial roles in the uptake, translocation, and storage of inorganic nitrogen in marine phytoplankton (see review in Rogato et al. 2015 and references therein, Glibert et al. 2016, Busseni et al. 2019). In general, most *Nrt2* and *Amt1* genes are highly expressed under nitrogen deficiency but repressed by the presence of ammonium (Hildebrand & Dahlin 2000, Hildebrand 2005, Kang et al. 2007, 2009, Song & Ward 2007, McDonald et al. 2010, Bender et al. 2014, Levitan et al. 2015, Kang & Rynearson 2019). Since these genes are rapidly and sensitively regulated in response to nitrogen status, they were proposed as potential nitrogen marker genes (Hildebrand & Dahlin 2000, Kang et al. 2007, Ashworth et al. 2013, Rogato et al. 2015, Suzuki et al. 2019). With the advancement of sequencing technology, transcriptomic studies have revealed comprehensive gene expression profiles of nitrogen metabolic pathways in response to nitrogen stresses, and *Nrt2* and *Amt1* genes often exhibit significant changes in differential expression analysis among different treatments (Allen et al. 2011, Ashworth et al. 2013, Bender et al. 2014, Harke et al. 2017, Lampe et al. 2018, Smith et al. 2019, Lampe et al. 2021). Applying this strategy to natural assemblages, metatranscriptomics has been found to be a powerful means to explore the *in situ* gene expression profiles among phytoplankton groups (Alexander et al. 2015, Caron et al. 2017, Lampe et al. 2018, Suzuki et al. 2019, Zhang et al. 2019, Shih et al. 2021). Therefore, metatranscriptomics should be a useful method for examining the individual gene transcriptional pattern of nitrogen marker genes, which provides *in situ* information for evaluating the individual nitrogen status in natural assemblages.

Herein, we employed the ^{15}N-tracer technique to measure the nitrogen uptake characteristics of different size-fractionated phytoplankton in the southern East China Sea (ECS). Cross-shelf cruises were conducted to visit different water masses, including coastal runoff, the Taiwan Warm Current (Shaw 1992), and a year-round upwelling system caused by the Kuroshio Current (Chern et al. 1990), which form a natural experimental field (see Fig. 1). The complex interactions with nitrogen supply stimulate different phytoplankton assemblages to thrive in this region (Kang et al. 2015). To evaluate the nitrogen status of phytoplankton, metatranscriptomes were generated to examine the individual gene expression of nitrogen transporter genes among different phytoplankton.

2. MATERIALS AND METHODS

2.1. Cruises and sampling

Three research cruises were carried out in the southern ECS on board the R/V 'Ocean Research II' in May 2018, July 2018, and June 2019. A cross-shelf

cruise track including 12 stations from the coastal zone of China to the Kuroshio Current was planned for sampling (see Fig. 1). The hydrographic parameters of temperature and salinity were measured with a CTD (SBE 911 plus, Sea-Bird Scientific). Seawater samples were collected with a rosette sampler equipped with 20 l Niskin bottles (General Oceanics). Samples for nutrient determination were quickly frozen in liquid nitrogen and then stored at −20°C until analysis. The concentration of nitrate was determined using the pink azo dye method with a detection limit of 0.3 µM (Gong 1992). Ammonium was analyzed using the modified indophenol blue method with a detection limit of 0.05 µM (Pai et al. 2001). Phosphate was measured by a modified molybdenum blue method with a detection limit of 0.01 µM (Liu et al. 2010). Chlorophyll *a* (chl *a*) concentrations were determined fluorometrically by the nonacidification method (Strickland & Parsons 1972). Water samples were prefiltered through 200 or 20 µm mesh screens and then collected with a GF/F filter (25 mm, Whatman). The chl *a* concentration of 20–200 µm cells, termed microphytoplankton here, was obtained by subtracting the data for cells <20 µm, termed pico-nanophytoplankton here, from the total chl *a* (cells <200 µm). Pico-nanophytoplankton samples for cell counting were collected from surface water prefiltered through a 20 µm mesh screen, preserved with paraformaldehyde (0.2% final concentration), and frozen in liquid nitrogen. Enumeration of pico-nanophytoplankton was performed based on cell size (forward- and side-scattering) and autofluorescence in the ranges of orange from phycoerythrin (575 ± 15 nm, for *Synechococcus*) and red from divinyl chlorophyll (>670 nm, for *Prochlorococcus* and photosynthetic picoeukaryotes) using a FACS Aria Flow Cytometer (Becton Dickinson) equipped with a 488 nm excitation laser. Microphytoplankton samples for cell counting were collected from surface water (5 m depth), preserved with acidic Lugol's solution, and counted using Sedgewick-Rafter couniting slides (Hausser Scientific) with a Nikon Optiphot 2 microscope at a magnification of 100×.

2.2. Determination of uptake rates and kinetic parameters

To determine the nitrogen uptake parameters from natural phytoplankton populations, ^{15}N uptake experiments were carried out during the day at Stn 1, Stn 5, and Stn 11 in May 2018; Stn 1 and Stn 9 in July 2018; and Stn 1 in June 2019. Surface water samples (5 m) were prefiltered through a 200 µm mesh screen. The samples were dispensed into 2 l polycarbonate bottles. Six concentrations (0.5, 1, 2, 5, 10, and 20 µM) of ^{15}N-nitrate or ^{15}N-ammonium were prepared by dilution from the stock solution ($Na^{15}NO_3$ and $^{15}NH_4Cl$, $^{15}N \geqslant 98$ atom %, Sigma-Aldrich). Each bottle was divided into 2 subsamples, and then one subsample was filtered immediately through a 20 µm mesh screen to remove microphytoplankton. All subsamples were dispensed into 500 ml polycarbonate bottles and incubated at 23 ± 1°C with a light intensity of 115 µE m^{-2} s^{-1} for 4–6 h (Dugdale & Wilkerson 1986). After incubation, the particulate matter was collected simultaneously in duplicate on GF/F filters with gentle suction, and the filtration volume was recorded. The filters were stored at −20°C and then completely dried in a vacuum desiccator. In the laboratory, the filters were dried in an oven at 60°C for 2 h and then packaged into a tin capsule. Pelletized capsules were analyzed using an elemental analyzer (Flash 2000, Thermo Scientific) coupled to an isotope ratio mass spectrometer (Finnigan MAT253, Thermo Scientific) for nitrogen content and isotopic composition. The nitrogen content was corrected using standard curves bracketing anticipated sample masses that were run prior to the samples using the protein standard OAS (Thermo Scientific) as a laboratory standard. The measured nitrogen isotopic composition was calibrated using protein standard OAS and USGS40 (L-glutamic acid: $\delta^{15}N = -4.5 \pm 0.1$‰; $w_N = 9.5$%; obtained from the international Atomic Energy Agency) into all runs at regular intervals (once every 8 analyses) for data calibration. Specific nitrate and ammonium uptake rates, V (units, h^{-1}), and absolute uptake rates, ρ (units, µmol N l^{-1} h^{-1}) were calculated according to the equations described by MacIsaac & Dugdale (1972) and Paasche & Kristiansen (1982):

$$V = \frac{\text{AT excess of product}}{\text{AT enrichment of substrate} \times \text{time}} \quad (1)$$

$$\rho = V \times \text{PON} \quad (2)$$

where 'AT% excess of product' is the atom % ^{15}N in the particulate sample, 'AT% enrichment of substrate' is the atom % ^{15}N in dissolved ammonium or nitrate as calculated from ambient and added concentration, and PON is the concentration of particulate organic nitrogen. The uptake rates of 20–200 µm cells were obtained by subtracting the absolute rates for cells <20 µm from those for cells <200 µm. Chl *a*-specific nitrogen uptake rates, ρ^{chl} (units, µmol N [µg chl *a*]$^{-1}$ h^{-1}), were calculated by normalizing the absolute uptake rates to the concentration of chl *a* following

the suggestion from Legendre & Gosselin (1997). The chl *a* concentrations of 2 size-fractionated phytoplankton were calculated from the pre-incubation water according to the filtration volume. The best-fit results of the uptake curve and kinetic parameter, ρ_{max}^{chl}, were obtained using nonlinear regression with the Michaelis-Menten equation by Dynamic Fit Wizard in SigmaPlot 14.5 (Systat):

$$\rho^{chl} = \frac{\rho_{max}^{chl}(S + S')}{K_s + (S + S')} \quad (3)$$

where S is the concentration of preexisting nitrogen, S' is the concentration of added tracer, ρ_{max}^{chl} is the maximum uptake rate, and K_s is the half-saturation constant.

2.3. Total RNA isolation and metatranscriptome sequencing

High-throughput sequencing was performed to obtain metatranscriptomes at Stn 1 in July 2018. Microplankton samples were collected using a 20 µm mesh plankton net with a mouth diameter of 0.5 m. An oblique tow was performed for 10 min at depths ranging from 0 to 5 m with the ship speed set to 1 knot. The collected samples were subsequently sieved through a 200 µm mesh screen to remove larger zooplankton and mesoplankton. A part of the processed microplankton sample was filtered through a 20 µm mesh screen and fixed with RLT buffer (Qiagen) and 1% β-mercaptoethanol. Two such subsamples were immediately stored in liquid nitrogen and labeled 'untreated samples'. To provide a relative criterion of nitrogen transporter gene transcript range for field species, the remaining processed microplankton samples were divided into 2 treatments for the incubations of the relative expression assay (Kang et al. 2009). Aliquots of 200 ml microplankton samples were placed in separate bottles containing 1.8 l of ammonium addition or N-free media prepared with artificial seawater. One treatment (ammonium addition) composed of 2 subsamples was treated with 100 µM ammonium for 1 h to stimulate the minimal transcript levels of nitrogen transporter genes from field assemblages. The other treatment (nitrogen-free) composed of 2 subsamples was incubated for 24 h in nitrogen-free f/20 media to stimulate the maximal transcript levels of nitrogen transporter genes from field assemblages. These nitrogen-manipulated subsamples were incubated at 23 ± 1°C with a light intensity of 115 µE m^{-2} s^{-1}. At the end of the incubation, the microplankton cells in each sample were collected and stored in the same way as the untreated samples. In the laboratory, the microplankton samples preserved with the RLT buffer were disrupted by supersonic treatment (VCX600, Sonics & Materials). Total RNA was isolated using an RNeasy Plant Mini Kit (Qiagen) according to the manufacturer's instructions. The RNase-free DNase I set (Qiagen) was used to remove the residual genomic DNA. The concentration of isolated RNA was determined using a spectrophotometer (ND-1000, NanoDrop Technologies). For metatranscriptomes, an aliquot of 5 µg total RNA was taken from each sample, and mRNA was purified using oligo (dT) polyA selection. The eluted mRNA was fragmented and reverse-transcribed into cDNA. After second-strand cDNA synthesis, specific adapters were ligated to both ends, and these cDNA fragments were ready for bridge PCR amplification (Illumina 2017). Metatranscriptome sequencing was performed by Genomics (New Taipei City, Taiwan) using an Illumina MiSeq system. Raw sequence data have been deposited in the NCBI database under accession number PRJNA799459.

2.4. Sequence analysis and taxonomic assignment

In the metatranscriptomes, low-quality reads and adapters were removed by fastp version 0.22.0 software (Chen et al. 2018) with default settings. Next, the ribosomal RNA sequences were filtered out by SortMeRNA version 4.3.4 software (Kopylova et al. 2012) against the Silva rRNA database version 138.1 (Quast et al. 2013). After removing adapters and rRNA, the remaining reads were set as clean reads. The Tara Oceans Eukaryote Gene Catalog (MATOU version 1; https://www.genoscope.cns.fr/tara/localdata/data/Geneset-v1/MATOU-v1.fna.gz) (Carradec et al. 2018) was indexed with Salmon version 1.5.2 software (Patro et al. 2017) using *k*-mers of length 31. Then, the clean reads were mapped to the index, and transcripts per kilobase million (TPM) values were calculated by Salmon using the quasimapping mode and the '—validateMappings' option.

According to the taxonomic affiliations table (https://www.genoscope.cns.fr/tara/localdata/data/Geneset-v1/taxonomy.tsv.gz), the lineage of the mapped genes were classified as unknown (not found in the taxonomy table), root (unigenes that match at least 2 of the Eukaryota, *Archaea*, *Bacteria*, and Virus superkingdoms), bacteria, O/U Eukaryota (where O/U represents unigenes for which taxonomic affiliation ended at the indicated level or belonged to minor classes of the affiliation), O/U Metazoa, O/U Deu-

terostomia, Tunicata, O/U Protostomia, Copepoda, Rhizaria, O/U Alveolata, Ciliophora, Dinophyceae, Chlorophyta, O/U Stramenopiles, Dictyochophyceae, Bacillariophyta, Pelagophyceae, and Haptophyceae. Hence, the proportion of TPM values in each lineage was also calculated.

2.5. Relative transcript levels of nitrogen transporter genes

To interpret the *in situ* (untreated) transcript abundance of the *Nrt2* and *Amt1* genes among different diatom genera, a relative expression assay (Kang et al. 2009) was applied to establish the range of variation for each nitrogen transporter gene from ammonium addition and nitrogen-free treatments. The reads mapped to the *Nrt2* and *Amt1* genes and their TPM values were subtracted from the metatranscriptomes under Bacillariophyta (diatoms), and the results classified under the same genera were combined. To test for differences in the means of TPM values of duplicate experiments from untreated samples and nitrogen-manipulated treatments, ANOVA and post hoc Tukey's test were used. Differences were considered statistically significant at $p < 0.05$.

3. RESULTS

3.1. Hydrology background

Among the sampling stations (Fig. 1) during the 3 cruises, Stn 1 was located near the coast of China, where relatively lower salinity levels and temperatures and higher nutrient concentrations were observed (Table 1). Among the 3 cruises, that in July 2018 detected the highest concentration of nitrate at 2.4 µM. By contrast, Stn 5 was located in the middle of the continental shelf, where a higher surface water temperature was detected during the May 2018 cruise. This station was affected by the Taiwan Warm Current, which is oligotrophic in nature (Shaw 1992). The surface concentrations of nitrate and phosphate were both lower than the detection limits (Table 1). Both Stn 9 and Stn 11 were located off the northeastern corner of Taiwan and were close to the upwelling center (near Stn 10; Fig. S1 in the Supplement at www.int-res.com/articles/suppl/m726p017_supp.pdf). During the cruises in 2018, more obvious upwelling was observed in May based on the contour maps of water temperature and salinity (Fig. S1).

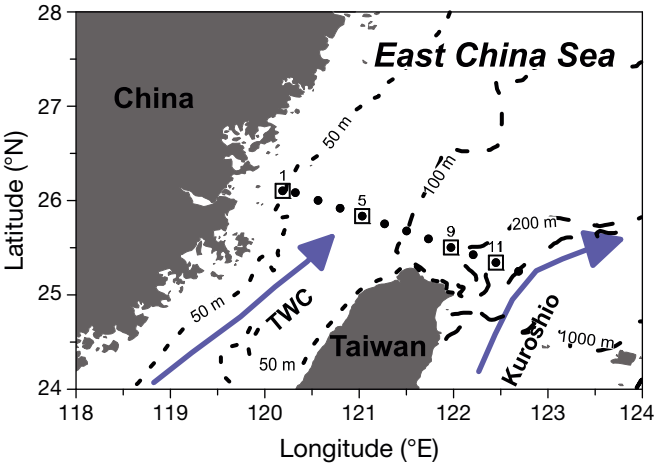

Fig. 1. Sampling stations in the southern East China Sea, with depth contours shown. Points: sampling stations on the transect line; black squares: stations for which ^{15}N uptake experiments were conducted. A schematic shows the surface circulation in the summertime. TWC: Taiwan Warm Current; Kuroshio: Kuroshio Current

3.2. Chl *a* concentration and phytoplankton composition

Relatively high total chl *a* concentrations ranging from 0.73 to 1.31 µg l^{-1} were observed at Stn 1 near the coast and Stns 9 and 11 close to the upwelling center (Table 1). Both size-fractionated (<20 and 20–200 µm) chl *a* concentrations were detected for pico-nanophytoplankton and microphytoplankton within the same station. Flow cytometry analysis indicated that *Synechococcus* generally dominated the cyanobacteria communities except at Stn 1 in July 2018, when *Prochlorococcus* dominated the community. The cell counts of microphytoplankton ranged between 4.1×10^3 and 180×10^3 cells l^{-1}, and diatoms were the dominant group, comprising over 88% of the microphytoplankton communities (Table 1). At Stn 5, the chl *a* concentration of pico-nanophytoplankton was 6 times higher than that of microphytoplankton, and flow cytometry analysis showed that *Prochlorococcus* was the dominant group (Table 1). The concentration of microphytoplankton was as low as 1.0×10^3 cells l^{-1}, and the relative abundance of dinoflagellates was slightly greater than that of diatoms.

3.3. Nitrogen uptake characteristics

The nitrogen uptake curves obtained from natural assemblages in the southern ECS were classi-

Table 1. Hydrographic and biological properties of surface water at stations for ^{15}N uptake experiments in the southern East China Sea. (–) Lower than the detection limit

	May 2018			July 2018		June 2019
	Stn 1	Stn 5	Stn 11	Stn 1	Stn 9	Stn 1
Longitude (°E)	120.1892	121.0322	122.4486	120.1905	121.9725	120.1775
Latitude (°N)	26.1031	25.8350	25.3422	26.0877	25.5028	26.0438
Temp (°C)	23.8	26.8	23.6	26.0	27.9	24.2
Salinity (psu)	34.2	34.3	34.4	33.6	33.9	31.7
NO_3^- (μM)	–	–	0.3	2.4	0.7	–
NH_4^+ (μM)	0.25	0.17	0.07	0.11	0.10	0.74
PO_4^{3-} (μM)	0.55	–	0.06	0.09	0.07	0.06
Chl *a*						
<200 μm (μg l^{-1})	0.77	0.30	1.15	0.73	0.83	1.31
20–200 μm (μg l^{-1})	0.29	0.04	0.67	0.38	0.19	0.40
<20 μm (μg l^{-1})	0.48	0.26	0.48	0.35	0.64	0.91
Flow cytometry						
Prochlorococcus (cells ml^{-1})	1.6×10^4	1.5×10^4	1.2×10^4	3.6×10^3	1.1×10^4	8.8×10^2
Synechococcus (cells ml^{-1})	6.5×10^4	4.4×10^3	2.9×10^4	1.8×10^3	1.4×10^5	2.5×10^4
Picoeukaryotes (cells ml^{-1})	2.2×10^4	2.9×10^3	8.1×10^3	4.2×10^3	1.5×10^4	4.5×10^2
Microscope						
Diatoms (cells l^{-1})	1.8×10^4	3.9×10^2	4.1×10^4	1.8×10^5	4.1×10^3	1.3×10^5
Dinoflagellates (cells l^{-1})	2.1×10^3	5.4×10^2	4.9×10^2	9.8×10^2	2.4×10^2	5.0×10^3

fied into 3 types (Fig. 2, Fig. S2 in the Supplement, Table 2). First, the curve matches the typical reaction trend described by the Michaelis-Menten model (Michaelis-Menten hyperbola with $r^2 > 0.25$). With the increase in added nitrogen, the uptake rates initially showed a linear increase and then reached a saturated level (Fig. 2A). Second, regardless of the amount of nitrogen addition, a constant uptake rate was obtained (Fig. 2B). Finally, the uptake rates of ammonium decreased with increasing ammonium addition (Fig. 2C). This type of uptake curve cannot generate ρ_{max}^{chl}, and the highest uptake rate was observed when the lowest ^{15}N was added.

Comparing the maximum nitrogen uptake rates detected in the southern ECS, the pico-nanophytoplankton ρ_{max}^{chl} of ammonium was significantly higher than that of nitrate (Fig. 3A, Table 2), indicating that pico-nanophytoplankton should have a relatively superior capacity to take up ammonium. By contrast, the maximum uptake rates for ammonium and nitrate were similar in the microphytoplankton (Fig. 3B). The ρ_{max}^{chl} of ammonium in pico-nanophytoplankton varied among the samples, but there was no significant difference in the ρ_{max}^{chl} of ammonium between pico-nanophytoplankton and microphytoplankton at the same station (Fig. 3C). However, the ρ_{max}^{chl} of nitrate in microplankton was significantly higher than that of pico-nanophytoplankton (Fig. 3D, Table 2). Interestingly, an exceptional case that did not match the overall uptake characteristics above was found in the microphytoplankton at Stn 1 in July 2018 (Figs. 3B,C,D, red lines). Therefore, metatranscriptomic analysis was performed to examine the *in situ* nitrogen status of microphytoplankton at Stn 1 in July 2018.

3.4. Analysis of metatranscriptomes

The raw reads of the metatranscriptomes ranged from 4.6×10^6 to 6.2×10^6 (Table S1 in the Supplement). After adapter trimming and rRNA removal, 30.2–75.1% of the clean reads were mapped with unigenes of MATOU version 1 (Table S1). Overall, a total of 19.4% (204 351 out of 1 054 568) of unigenes belonged to Bacillariophyta (Fig. 4A). Among the transcriptomes from the untreated samples and from 2 nitrogen-manipulated treatments, a high proportion of TPM with an average of 41% accounted for diatoms, which was consistent with the dominance of diatoms revealed by the microscopic counts (Table 1). Interestingly, the percentage of mapped reads for diatoms increased in the ammonium addition treatments but decreased in the nitrogen-free treatments (Fig. 4B).

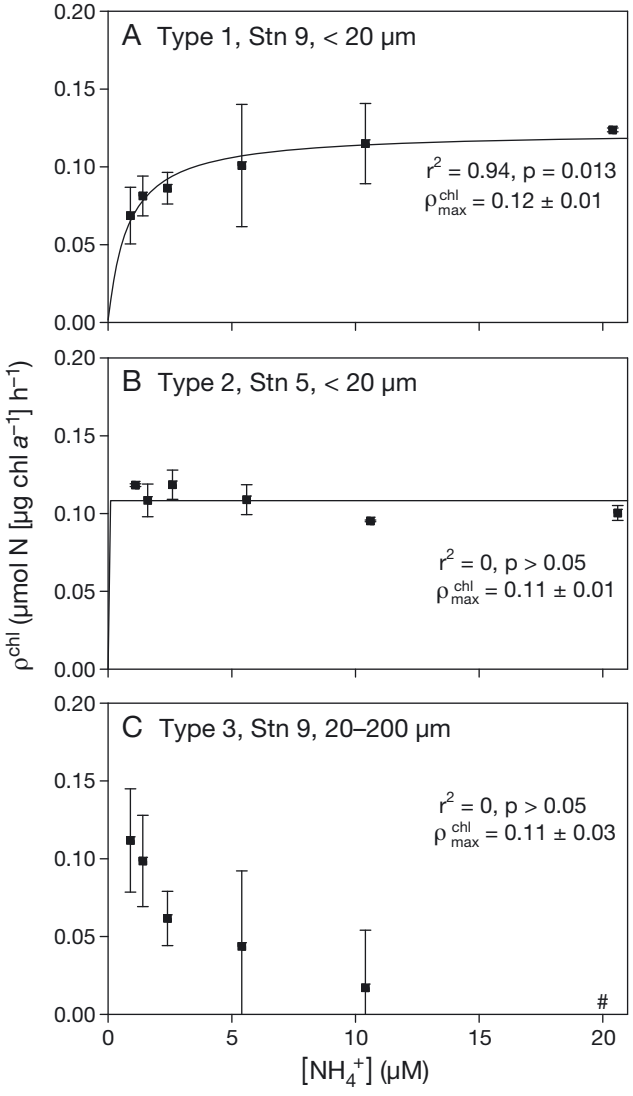

Fig. 2. Three types of nitrogen uptake curves observed in the surface water of the southern East China Sea. (A) Type 1, an example from the ammonium uptake curve of pico-nanophytoplankton at Stn 9 in July 2018. (B) Type 2, an example from the ammonium uptake curve of pico-nanophytoplankton at Stn 5 in May 2018. (C) Type 3, an example from the ammonium uptake curve of microphytoplankton at Stn 9 in July 2018. Error bars: ±SD from 3 replicate samples. (#) No uptake rate was detected

To evaluate the nitrogen status of diatoms, the gene expression of nitrogen transporters was extracted and compared among 4 common genera, *Chaetoceros*, *Leptocylindrus*, *Pseudo-nitzschia*, and *Thalassionema*, found in these metatranscriptomes (Fig. 5). To establish the transcript criteria for *Nrt2* and *Amt*1 gene expression in natural assemblages, relative expression assays were conducted to reduce the transcript level with the ammonium-addition treatments or to induce high transcript levels in the nitrogen-free treatments. Higher transcriptional levels in the nitrogen-free treatments than in the ammonium addition treatments were found in both genes; however, statistically significant changes were only obtained in the *Nrt2* gene (Fig. 5). The *Nrt2* transcript levels of overall diatoms, *Chaetoceros*, and *Thalassionema* in the untreated samples were as low as those in the ammonium-addition treatments, indicating that most diatoms should be in a nitrogen status in which the expression of nitrate transporter genes was repressed.

Table 2. Comparison of the maximum uptake rates of nitrate and ammonium in the pico-nanophytoplankton (<20 µm) and microphytoplankton (20–200 µm) at surface waters in the southern East China Sea. ND: the added ammonium was taken up by the pico-nanophytoplankton, and only the ammonium uptake rate for pico-nanophytoplankton was detected

		20–200 µm ρ^{chl}_{max} (µmol N [µg chl *a*]$^{-1}$ h^{-1})		<20 µm ρ^{chl}_{max} (µmol N [µg chl *a*]$^{-1}$ h^{-1})	
		NH_4^+	NO_3^-	NH_4^+	NO_3^-
May 2018	Stn 1	0.05 ± 0.01[a]	0.11 ± 0.02	0.06 ± 0.01[b]	0.02 ± 0.01[a]
	Stn 5	0.11 ± 0.03[b]	0.04 ± 0.01[b]	0.11 ± 0.01[b]	0.01 ± 0.01[a]
	Stn 11	0.11 ± 0.02[b]	0.10 ± 0.02	0.20 ± 0.01[b]	0.04 ± 0.01[a]
July 2018	Stn 1	ND	0.03 ± 0.01[a]	0.33 ± 0.02[a]	0.09 ± 0.01[a]
	Stn 9	0.11 ± 0.03[c]	0.05 ± 0.01[b]	0.12 ± 0.01[a]	0.01 ± 0.01[b]
June 2019	Stn 1	0.14 ± 0.04[b]	0.10 ± 0.02	0.41 ± 0.02	0.10 ± 0.02[a]

[a]Type 1 uptake curve; [b]Type 2 uptake curve; [c]Type 3 uptake curve. Uptake curve cannot fit to the Michaelis-Menten function and ρ^{chl}_{max} is the uptake rate under the lowest ^{15}N addition

4. DISCUSSION

^{15}N tracer techniques for natural assemblages can provide valuable information for evaluating the nitrogen uptake capacities of natural phytoplankton. Considering that phytoplankton can regulate the number of nutrient transporters to cope with changes in nutrient availability (Aksnes & Egge 1991, Smith et al. 2009, Bonachela et al. 2011), the uptake parameter ρ^{chl}_{max} should indicate the capacity of the nutrient uptake system, which reflects the adaptation of phytoplankton to the ambient environment. In the southern ECS, the ρ^{chl}_{max} for ammonium estimated from the pico-

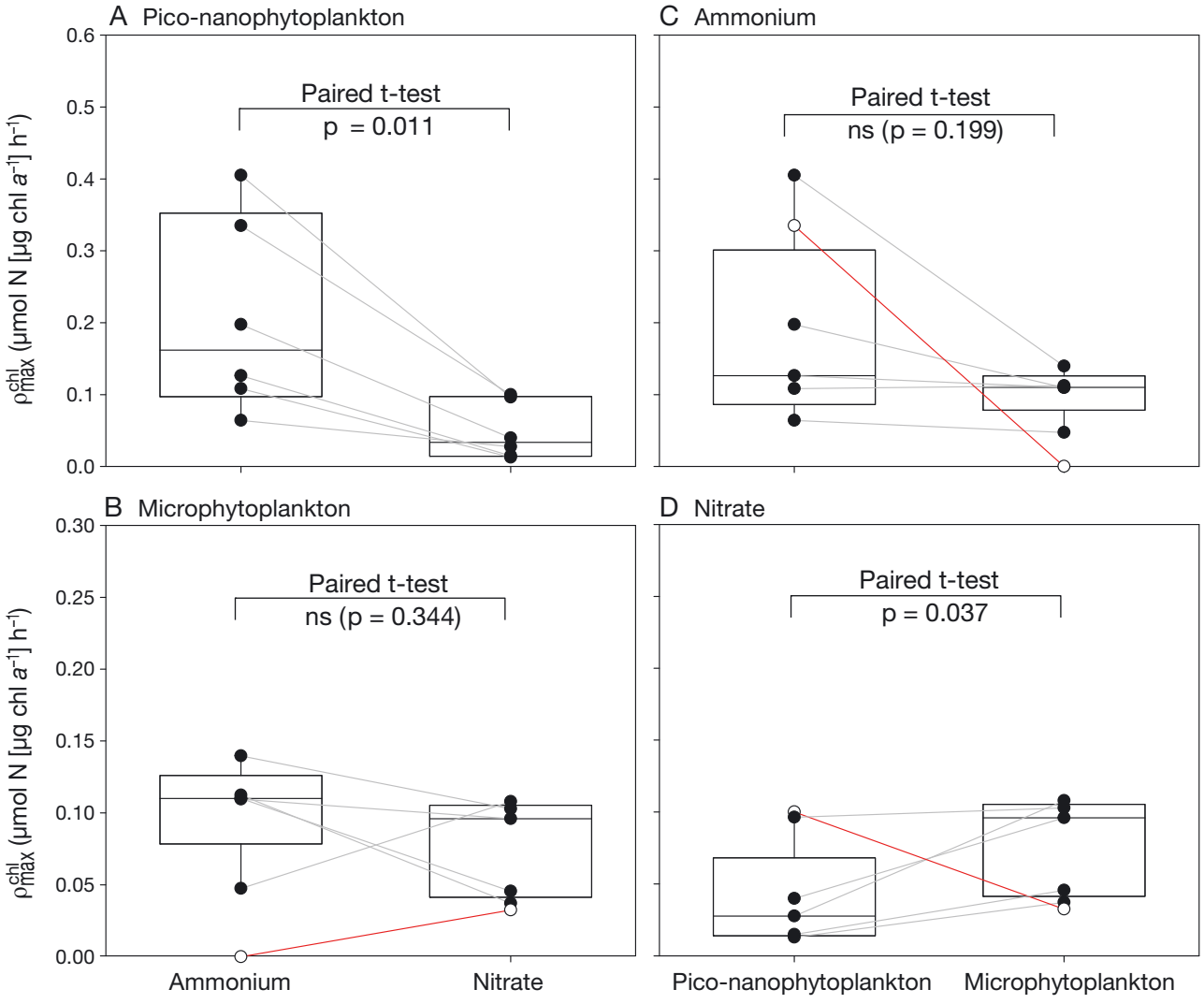

Fig. 3. Comparison of nitrogen maximum uptake rates between pico-nanophytoplankton and microphytoplankton from the southern East China Sea during 3 cruises. Paired *t*-test results of maximum uptake rates of ammonium and nitrate in (A) pico-nanophytoplankton from the same station and (B) microphytoplankton from the same station. Paired *t*-test results of maximum (C) ammonium uptake rates between pico-nanophytoplankton and microphytoplankton from the same station and (D) nitrate uptake rates between pico-nanophytoplankton and microphytoplankton from the same station. The 'ND' result of ammonium uptake measured in microphytoplankton at Stn 1 in July 2018 was visualized as zero in (B) and (C). Data points marked by open circles connected with a red line were excluded from the paired *t*-test. ns: not significant

nanophytoplankton was usually higher than that for nitrate (Table 2). By contrast, microphytoplankton possess a similar ρ_{max}^{chl} for ammonium and nitrate, and the ρ_{max}^{chl} of nitrate in microphytoplankton was usually higher than that of pico-nanophytoplankton at the same station (Table 2). These results were generally consistent with the nitrate and ammonium uptake characteristics of phytoplankton from the literature in culture experiments and field observations (Glibert et al. 2016 and references therein). However, the field environments were much more complex than the controlled laboratory settings. For example, the uptake rates detected for microphytoplankton should be a result of competition with pico-nanophytoplankton according to our experimental procedures in this study. Indeed, almost half of the uptake curves did not match the typical Michaelis-Menten uptake curves (Table 2). These results indicated that the uptake parameters detected from natural assemblages reflected their *in situ* uptake characteristics, which were influenced by their physiological states and environmental factors.

To compare nitrogen uptake rates from natural assemblages across different sampling times and loca-

tions, it is essential to calculate phytoplankton-specific N uptake rates by normalizing ^{15}N PON uptake to phytoplankton biomass. Normalizing nitrogen uptake rates to chl *a* has been recommended for nitrogen uptake estimation in natural samples (Dickson & Wheeler 1995, Legendre & Gosselin 1997), but the use of chl *a* as an estimator of phytoplankton biomass has been criticized due to changes in the amount of chl *a* per cell affected by irradiance and growth conditions. As uptake rates are influenced by the cell surface (Edwards et al. 2012, Marañón et al. 2013), using biovolume as a normalization basis for phytoplankton biomass is a more suitable approach. Recently, the integration of automated imaging analysis systems complemented by chl *a* fluorescence detection has been proposed as a promising method for estimating phytoplankton biomass (Menden-Deuer et al. 2020, Owen et al. 2022). Incorporating such systems for phytoplankton biovolume and/or biomass estimation, combined with ^{15}N tracer techniques, would enhance the accuracy of phytoplankton-specific nitrogen uptake rate estimation, particularly in the context of temporal and spatial variations.

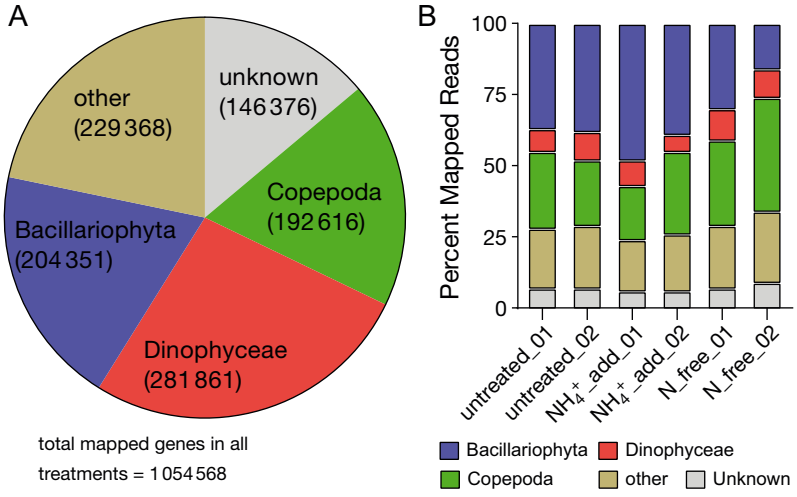

Fig. 4. Taxonomic distribution of mapped unigenes from metatranscriptomes for microphytoplankton at Stn 1 in July 2018 showing (A) total mapped unigenes and (B) percentage of mapped reads in each treatment (2 replicates). Unknown: unigenes that have no similarities in amino databases, Tara MATOU version 1 catalog definition; Other: taxonomic groups not belonging to Bacillariophyta, Dinophyceae, Copepoda, and unknown; Treatments: NH_4^+_add: ammonium addition; N_free: nitrogen-free

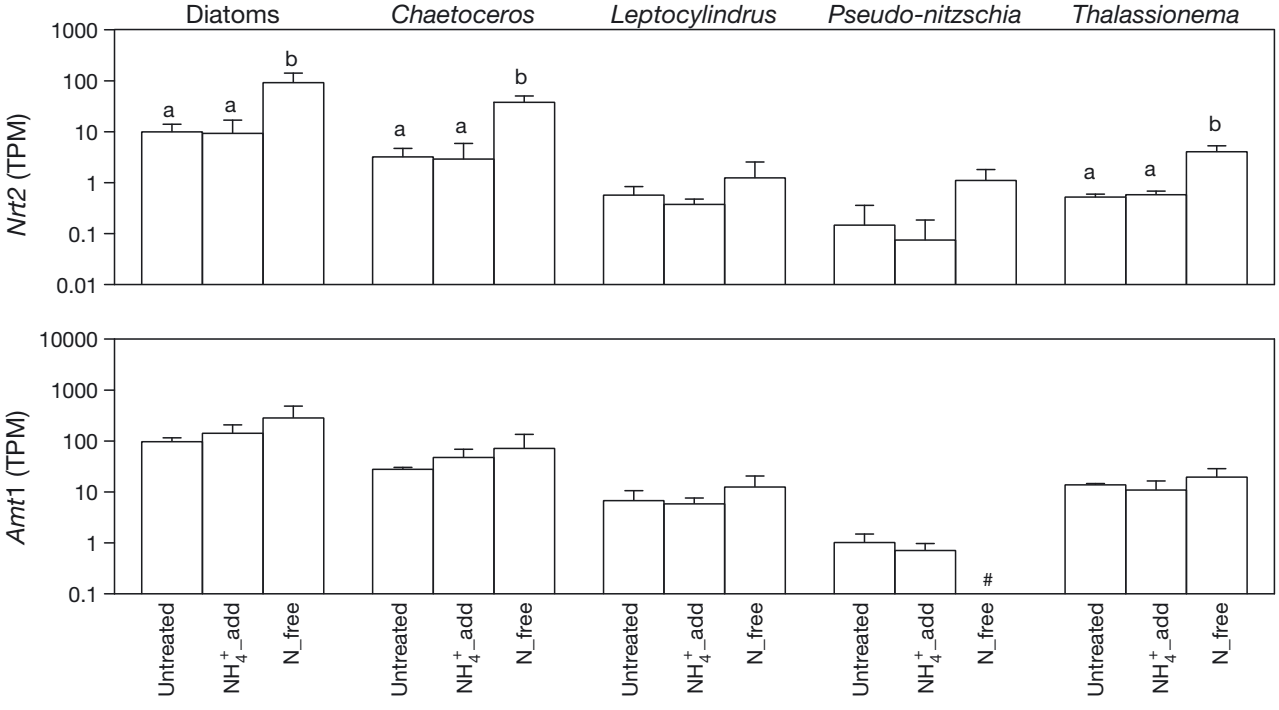

Fig. 5. Comparison of the expression levels of the *Nrt2* and *Amt1* genes among different diatom genera at Stn 1 in July 2018. The *in situ* (untreated) transcripts per million (TPM) value was compared to that from ammonium addition (NH_4^+_add) and nitrogen-free (N_free) treatments. The same letters above the columns indicate no significant difference between means of TPM ($p < 0.05$, ANOVA with Tukey's test). Error bars: ±1 SD of duplicate experiments. (#) No reads were detected

Three types of nitrogen uptake curves were detected in the southern ECS (Figs. 2 & S2). In general, typical Michaelis-Menten uptake curves were obtained in nutrient-deficient cultures (e.g. Dortch et al.1982, Harrison et al. 1989). In this study, uptake curves fitting the Michaelis-Menten equation (Type 1, with $r^2 > 0.25$) were often detected in most of the nitrate uptake experiments of pico-nanophytoplankton (Fig. S2, Table 2). Interestingly, both nitrate and ammonium uptake curves matched the Type 1 curves and were detected only for the pico-nanophytoplankton at Stn 1 in July 2018 (Fig. S2O,P). This result indicates that pico-nanophytoplankton could have been under nitrogen-deficient conditions at Stn 1 in July 2018. In addition, a relatively higher ρ_{max}^{chl} value for ammonium than that from other stations was obtained (Table 2), which is consistent with phytoplankton possessing the ability to enhance the maximum uptake rate under nitrogen stress (McCarthy & Goldman 1979, Syrett et al. 1986).

Regarding the nontypical uptake curves, a Type 2 uptake curve with a constant uptake rate was generated by nonlinear regression. This type of uptake curve was also reported in other field investigations and considered as cells being limited by factors other than the substrate (MacIsaac & Dugdale 1969, Shiomoto et al. 1994). Half of the uptake curves detected in the southern ECS were classified as Type 2 curves, and a relatively lower ρ_{max}^{chl} for nitrate or ammonium compared to that from Type 1 uptake curves was obtained (Table 2). These results might have been due to our lowest assayed nutrient concentrations being higher than the ambient concentrations, and the nitrogen uptake rates would have been saturated within the lowest injected substrate concentration, especially at the stations with small phytoplankton populations. However, the Type 2 curves detected at phytoplankton-rich stations imply that the nitrogen uptake rates were limited by factors other than the concentrations of nitrate or ammonium in the studied region. In addition, the Type 3 uptake curve was a result of ammonium repression, in which ammonium generated a feedback inhibition effect on the uptake of ammonium or nitrate (Glibert & Goldman 1981, Dortch 1990, Flynn et al. 1997, Lomas & Glibert 1999). It has been proposed that ammonium or its assimilation products act as repressors of ammonium transport (Flynn et al. 1997). The most representative case of ammonium repression in nitrogen uptake was observed in microphytoplankton at Stn 9 in July 2018 (Fig. 2C). Based on the low ρ_{max}^{chl} of ammonium and nitrate for both pico-nanophytoplankton and microphytoplankton at Stn 9 in July 2018, nitrogen should not be the limiting nutrient at this station.

An exceptional case in which the uptake parameters did not match the general uptake characteristics above was found in the microphytoplankton at Stn 1 in July 2018 (Fig. 3B,C,D, red lines). The amount of ^{15}N-ammonium uptake measured from the pico-nanophytoplankton (<20 μm) was slightly greater than or equal to that from the whole phytoplankton community (<200 μm) (Fig. S3 in the Supplement), which indicated that most of the added ^{15}N ammonium was quickly taken up by the pico-nanophytoplankton. This result was consistent with not only pico-nanophytoplankton being successful competitors for ammonium uptake but also pico-nanophytoplankton having the capacity for rapid ammonium uptake under the nitrogen deficiency conditions discussed above. According to the results of the chl *a* analysis and counting under a microscope, there was a relatively high abundance (1.8×10^3 cells l^{-1}) of microphytoplankton at Stn 1 in July 2018. Although the ambient concentration of ammonium in the surface water was low, there was a relatively high concentration of nitrate (2.4 μM). However, both the uptake rates of ammonium and nitrate for microphytoplankton were extremely low or undetectable (Table 2). Apparently, the ^{15}N uptake assay alone did not explain which nitrogen form supported the high abundance of microphytoplankton.

Metatranscriptomics is a promising method that simultaneously provides the overall gene expression from various species in an environmental sample. In theory, metatranscriptomes with sufficient sequencing depth could obtain all the transcript reads from the whole community, consisting of the composition of assemblages and their gene expression. In this study, the TPM method was used to normalize the gene reads to the whole community (Patro et al. 2017), and the TPM values were influenced by the composition of diatom assemblages in the samples. Four diatom genera, *Chaetoceros*, *Leptocylindrus*, *Pseudo-nitzschia*, and *Thalassionema*, were identified with TPM values for statistical analysis among the treatments (Fig. 5). With these genera also counted under a microscope (data not shown), the results indicated that these 4 genera were the major components in the diatom assemblages at Stn 1 in July 2018.

Since the TPM values were influenced by community composition, a suitable analysis process was necessary to interpret the gene transcript levels among the different diatom groups. Thus, in this study, we assumed that if the community composition did not vary during short-term incubations and the metatranscriptomes consisted of most constitutive transcripts from the same assemblage, the induced or repressed

transcript levels would provide relative criteria for gene expression range using the strategy of the relative expression assay (Kang et al. 2009). For the nitrogen transporter genes, the *Nrt2* gene showed a significant change between the ammonium addition and nitrogen deficiency conditions compared to the response of the *Amt1* genes (Fig. 5). A more dramatic transcriptional change in *Nrt2* under different nitrogen conditions than that in *Amt1* has been reported from culture experiments (Kang et al. 2007, Smith et al. 2019). This is one of the advantages of *Nrt2*, which has been considered a better nitrogen indicator gene for nitrogen status (Kang et al. 2007, Rogato et al. 2015). By contrast, there are multiple forms of *Nrt2* and *Amt1* genes per genome in diatoms, and the *Amt1* family is generally more complex than the *Nrt2* family (Armbrust et al. 2004, Bowler et al. 2008, Bender et al. 2014, Rogato et al. 2015). Since not all of the genes in a family exhibit the same transcriptional pattern in response to nitrogen conditions (Kang & Rynearson 2019), combining the gene expression of multiple forms in a family would average down the individual transcriptional patterns. To date, most metatranscriptomic studies have used next-generation sequencing platforms to obtain an enormous number of short reads. Due to the limited reference database for marine phytoplankton and the short sequencing length, it is still a challenging task to distinguish the gene expression of individual gene forms from different species. Nanopore direct RNA sequencing is a potential method to overcome the drawback of short reads (Garalde et al. 2018, Jain et al. 2022). In this study, overall *Nrt2* gene expression showed significant changes between the nitrogen deficiency and ammonium addition treatments, which indicated that the mRNA abundance of *Nrt2.1* should be the dominant form of *Nrt2* genes detected in our metatranscriptomes (Kang & Rynearson 2019). In addition, the *in situ* (untreated) *Nrt2* gene expression was as low as the level in the ammonium addition treatments (Fig. 5), indicating that most diatoms at Stn 1 in July 2018 stopped nitrate uptake and still utilized ammonium as a nitrogen source.

In the southern ECS, Stn 1 was located in the coastal region close to mainland China, which is a relatively complex environment influenced by river discharge, coastal upwelling, and currents. A time series field investigation in the Matsu Archipelago near Stn 1 showed that chl *a* concentrations increased with higher nutrient input during the flood season (April to June), and then the abundance of diatoms decreased dramatically with low ambient nutrient concentrations in the summertime (Tsai et al. 2018). In July 2018, the relatively low *Synechococcus* abundance in cyanobacteria with typical Type 1 ammonium and nitrate uptake curves of pico-nanophytoplankton suggested that pico-nanophytoplankton could be under nitrogen-limited conditions. With the presence of nitrate in the surface water, we originally suggested that microphytoplankton should use nitrate as a nitrogen source despite the low nitrate uptake rate detected from microphytoplankton. Surprisingly, our metatranscriptomic analysis indicated that diatoms should utilize ammonium before nitrate as a nitrogen source (Fig. 5). This result conflicted with the lack of uptake of ^{15}N ammonium detected for microphytoplankton (Table 2). Metatranscriptomic analysis also demonstrated that *Chaetoceros*, *Leptocylindrus*, *Pseudo-nitzschia*, and *Thalassionema* had become the major components of the diatom community instead of *Skeletonema*, which was considered the common dominant species on the coast of the ECS (Kang et al. 2015). Our previous field investigations using *Nrt2* as a nitrogen marker gene suggested that *Chaetoceros* tends to utilize ammonium as a nitrogen source (Kang et al. 2015, Shih et al. 2021). Recently, the use of secondary ion mass spectrometry with stable isotopic tracer incubations demonstrated that *Chaetoceros* should possess the ability to rapidly utilize regenerated ammonium under nitrogen-poor environments (Klawonn et al. 2019, Olofsson et al. 2019). Therefore, one of the plausible explanations would be that under nitrogen-limited conditions, regenerated ammonium was produced and consumed at balanced rates and pico-nanophytoplankton were acclimated to form more efficient uptake systems, depleting ambient ammonium as well as added ^{15}N ammonium. Microphytoplankton such as *Chaetoceros* should still rely on regenerated ammonium before nitrate to maintain their dominance in the later phase of blooms even if they have to compete for regenerated ammonium with pico-nanophytoplankton. It would require further evidence to explain the distinct regulations of nitrogen uptake among different size-fractionated phytoplankton in natural assemblages. These results also demonstrated that simultaneously considering physiological states and nutrient uptake kinetics provides more comprehensive information to understand how phytoplankton cope with environmental changes.

Acknowledegments. This study was supported by a research grant from the National Science and Technology Council ROC (MOST 109-2628-M-019-001-MY4). C.Y.S. was supported by an NSTC postdoctoral fellowship (MOST 112-2811-M-019-002).

LITERATURE CITED

Aksnes DL, Egge JK (1991) A theoretical model for nutrient uptake in phytoplankton. Mar Ecol Prog Ser 70:65–72

Alexander H, Jenkins BD, Rynearson TA, Dyhrman ST (2015) Metatranscriptome analyses indicate resource partitioning between diatoms in the field. Proc Natl Acad Sci USA 112:E2182–E2190

Allen AE, Dupont CL, Oborník M, Horák A and others (2011) Evolution and metabolic significance of the urea cycle in photosynthetic diatoms. Nature 473:203–207

Armbrust EV, Berges JA, Bowler C, Green BR and others (2004) The genome of the diatom *Thalassiosira pseudonana*: ecology, evolution, and metabolism. Science 306: 79–86

Ashworth J, Coesel S, Lee A, Armbrust EV, Orellana MV, Baliga NS (2013) Genome-wide diel growth state transitions in the diatom *Thalassiosira pseudonana.* Proc Natl Acad Sci USA 110:7518–7523

Bender SJ, Durkin CA, Berthiaume CT, Morales RL, Armbrust EV (2014) Transcriptional responses of three model diatoms to nitrate limitation of growth. Front Mar Sci 1:3

Bonachela JA, Raghib M, Levin SA (2011) Dynamic model of flexible phytoplankton nutrient uptake. Proc Natl Acad Sci USA 108:20633–20638

Bowler C, Allen AE, Badger JH, Grimwood J and others (2008) The *Phaeodactylum* genome reveals the evolutionary history of diatom genomes. Nature 456:239–244

Busseni G, Vieira FRJ, Amato A, Pelletier E and others (2019) Meta-omics reveals genetic flexibility of diatom nitrogen transporters in response to environmental changes. Mol Biol Evol 36:2522–2535

Caron DA, Alexander H, Allen AE, Archibald JM and others (2017) Probing the evolution, ecology and physiology of marine protists using transcriptomics. Nat Rev Microbiol 15:6–20

Carradec Q, Pelletier E, Da Silva C, Alberti A and others (2018) A global ocean atlas of eukaryotic genes. Nat Commun 9:373

Chen S, Zhou Y, Chen Y, Gu J (2018) fastp: an ultra-fast all-in-one FASTQ preprocessor. Bioinformatics 34:i884–i890

Chern CS, Wang J, Wang DP (1990) The exchange of Kuroshio and East China Sea shelf water. J Geophys Res 95: 16017–16023

Collos Y, Vaquer A, Souchu P (2005) Acclimation of nitrate uptake by phytoplankton to high substrate levels. J Phycol 41:466–478

Dickson ML, Wheeler PA (1995) Nitrate uptake rates in a coastal upwelling regime: a comparison of PN-specific, absolute, and chl *a*-specific rates. Limnol Oceanogr 40: 533–543

Dortch Q (1982) Effect of growth conditions on accumulation of internal nitrate, ammonium, amino acids, and protein in three marine diatoms. J Exp Mar Biol Ecol 61:243–264

Dortch Q (1990) The interaction between ammonium and nitrate uptake in phytoplankton. Mar Ecol Prog Ser 61: 183–201

Dortch Q, Clayton J, Thoreson S, Bressler S, Ahmed S (1982) Response of marine phytoplankton to nitrogen deficiency: decreased nitrate uptake vs enhanced ammonium uptake. Mar Biol 70:13–19

Downing JA, Osenberg CW, Sarnelle O (1999) Meta-analysis of marine nutrient-enrichment experiments: variation in the magnitude of nutrient limitation. Ecology 80: 1157–1167

Dugdale RC, Wilkerson FP (1986) The use of ^{15}N to measure nitrogen uptake in eutrophic oceans; experimental considerations. Limnol Oceanogr 31:673–689

Edwards KF, Thomas MK, Klausmeier CA, Litchman E (2012) Allometric scaling and taxonomic variation in nutrient utilization traits and maximum growth rate of phytoplankton. Limnol Oceanogr 57:554–566

Eppley RW, Rogers JN, McCarthy JJ (1969) Half-saturation constants for uptake of nitrate and ammonium by marine phytoplankton. Limnol Oceanogr 14:912–920

Falkowski PG (1975) Nitrate uptake in marine phytoplankton: comparison of half-saturation constants from seven species. Limnol Oceanogr 20:412–417

Flynn KJ, Fasham MJR, Hipkin CR (1997) Modelling the interactions between ammonium and nitrate uptake in marine phytoplankton. Philos Trans R Soc Lond B 352: 1625–1645

Garalde DR, Snell EA, Jachimowicz D, Sipos B and others (2018) Highly parallel direct RNA sequencing on an array of nanopores. Nat Methods 15:201–206

Glibert PM, Goldman JC (1981) Rapid ammonium uptake by marine phytoplankton. Mar Biol Lett 2:25–31

Glibert PM, McCarthy JJ (1984) Uptake and assimilation of ammonium and nitrate by phytoplankton: indices of nutritional status for natural assemblages. J Plankton Res 6:677–697

Glibert PM, Wilkerson FP, Dugdale RC, Raven JA and others (2016) Pluses and minuses of ammonium and nitrate uptake and assimilation by phytoplankton and implications for productivity and community composition, with emphasis on nitrogen-enriched conditions. Limnol Oceanogr 61:165–197

Gong GC (1992) Chemical hydrography of the Kuroshio front in the sea northern to Taiwan. PhD dissertation, National Taiwan University, Taipei

Harke MJ, Juhl AR, Haley ST, Alexander H, Dyhrman ST (2017) Conserved transcriptional responses to nutrient stress in bloom-forming algae. Front Microbiol 8:1279

Harrison PJ, Parslow JS, Conway HL (1989) Determination of nutrient uptake kinetic parameters: a comparison of methods. Mar Ecol Prog Ser 52:301–312

Hildebrand M (2005) Cloning and functional characterization of ammonium transporter from the marine diatom *Cylindrotheca fusiformis* (Bacillariophyceae). J Phycol 41:105–113

Hildebrand M, Dahlin K (2000) Nitrate transporter genes from the diatom *Cylindrotheca fusiformis* (Bacillariophyceae): mRNA levels controlled by nitrogen source and by the cell cycle. J Phycol 36:702–713

Illumina (2017) TruSeq stranded mRNA reference guide. https://support.illumina.com/downloads/truseq-stranded-mrna-reference-guide-1000000040498.html

Jain M, Abu-Shumays R, Olsen HE, Akeson M (2022) Advances in nanopore direct RNA sequencing. Nat Methods 19:1160–1164

Kanda J, Saino T, Hattori A (1985) Nitrogen uptake by natural populations of phytoplankton and primary production in the Pacific Ocean: regional variability of uptake capacity. Limnol Oceanogr 30:987–999

Kang LK, Rynearson TA (2019) Identification and expression analyses of the nitrate transporter gene (*NRT2*) family among *Skeletonema* species (Bacillariophyceae). J Phycol 55:1115–1125

Kang LK, Hwang SPL, Gong GC, Lin HJ, Chen PC, Chang J (2007) Influences of nitrogen deficiency on the transcript

levels of ammonium transporter, nitrate transporter and glutamine synthetase genes in *Isochrysis galbana* (Isochrysidales, Haptophyta). Phycologia 46:521–533

Kang LK, Hwang SPL, Lin HJ, Chen PC, Chang J (2009) Establishment of minimal and maximal transcript levels for nitrate transporter genes for detecting nitrogen deficiency in the marine phytoplankton *Isochrysis galbana* (Prymnesiophyceae) and *Thalassiosira pseudonana* (Bacillariophyceae). J Phycol 45:864–872

Kang LK, Gong GC, Wu YH, Chang J (2015) The expression of nitrate transporter genes reveals different nitrogen statuses of dominant diatom groups in the southern East China Sea. Mol Ecol 24:1374–1386

Klawonn I, Bonaglia S, Whitehouse MJ, Littmann S and others (2019) Untangling hidden nutrient dynamics: rapid ammonium cycling and single-cell ammonium assimilation in marine plankton communities. ISME J 13:1960–1974

Kopylova E, Noé L, Touzet H (2012) SortMeRNA: fast and accurate filtering of ribosomal RNAs in metatranscriptomic data. Bioinformatics 28:3211–3217

Lampe RH, Cohen NR, Ellis KA, Bruland KW and others (2018) Divergent gene expression among phytoplankton taxa in response to upwelling. Environ Microbiol 20: 3069–3082

Lampe RH, Hernandez G, Lin YY, Marchetti A (2021) Representative diatom and coccolithophore species exhibit divergent responses throughout simulated upwelling cycles. mSystems 6:e00188-21

Legendre L, Gosselin M (1997) Estimation of N or C uptake rates by phytoplankton using ^{15}N or ^{13}C: revisiting the usual computation formulae. J Plankton Res 19:263–271

Levitan O, Dinamarca J, Zelzion E, Gorbunov MY, Falkowski PG (2015) An RNA interference knock-down of nitrate reductase enhances lipid biosynthesis in the diatom *Phaeodactylum tricornutum*. Plant J 84:963–973

Li J, Glibert PM, Zhou M (2010) Temporal and spatial variability in nitrogen uptake kinetics during harmful dinoflagellate blooms in the East China Sea. Harmful Algae 9: 531–539

Litchman E, Klausmeier CA, Schofield OM, Falkowski PG (2007) The role of functional traits and trade-offs in structuring phytoplankton communities: scaling from cellular to ecosystem level. Ecol Lett 10:1170–1181

Liu HC, Gong GC, Chang J (2010) Lateral water exchange between shelf-margin upwelling and Kuroshio waters influences phosphorus stress in microphytoplankton. Mar Ecol Prog Ser 409:121–130

Lomas MW, Glibert PM (1999) Interactions between NH_4^+ and NO_3^- uptake and assimilation: comparison of diatoms and dinoflagellates at several growth temperatures. Mar Biol 133:541–551

Lomas MW, Glibert PM (2000) Comparisons of nitrate uptake, storage, and reduction in marine diatoms and flagellates. J Phycol 36:903–913

MacIsaac JJ, Dugdale RC (1969) The kinetics of nitrate and ammonia uptake by natural populations of marine phytoplankton. Deep Sea Res Oceanogr Abstr 16:45–57

MacIsaac JJ, Dugdale RC (1972) Interactions of light and inorganic nitrogen in controlling nitrogen uptake in the sea. Deep-Sea Res 19:209–232

Marañón E, Cermeño P, López-Sandoval DC, Rodríguez-Ramos T and others (2013) Unimodal size scaling of phytoplankton growth and the size dependence of nutrient uptake and use. Ecol Lett 16:371–379

McCarthy JJ, Goldman JC (1979) Nitrogenous nutrition of marine phytoplankton in nutrient-depleted waters. Science 203:670–672

McDonald SM, Plant JN, Worden AZ (2010) The mixed lineage nature of nitrogen transport and assimilation in marine eukaryotic phytoplankton: a case study of *Micromonas*. Mol Biol Evol 27:2268–2283

McGlathery KJ, Pedersen MF, Borum J (1996) Changes in intracellular nitrogen pools and feedback controls on nitrogen uptake in *Chaetomorpha linum* (Chlorophyta). J Phycol 32:393–401

Menden-Deuer S, Morison F, Montalbano AL, Franze F and others (2020) Multi-instrument assessment of phytoplankton abundance and cell sizes in monospecific laboratory cultures and whole plankton community composition in the North Atlantic. Front Mar Sci 7:254

Olofsson M, Robertson EK, Edler L, Arneborg L, Whitehouse MJ, Ploug H (2019) Nitrate and ammonium fluxes to diatoms and dinoflagellates at a single cell level in mixed field communities in the sea. Sci Rep 9:1424

Owen BM, Hallett CS, Cosgrove JJ, Tweedley JR, Moheimani NR (2022) Reporting of methods for automated devices: a systematic review and recommendation for studies using FlowCam for phytoplankton. Limnol Oceanogr Methods 20:400–427

Paasche E, Kristiansen S (1982) Nitrogen nutrition of the phytoplankton in the Oslofjord. Estuar Coast Shelf Sci 14:237–249

Pai SC, Tsau YJ, Yang TI (2001) pH and buffering capacity problems involved in the determination of ammonia in saline water using the indophenol blue spectrophotometric method. Anal Chim Acta 434:209–216

Patro R, Duggal G, Love MI, Irizarry RA, Kingsford C (2017) Salmon provides fast and bias-aware quantification of transcript expression. Nat Methods 14:417–419

Quast C, Pruesse E, Yilmaz P, Gerken J and others (2013) The SILVA ribosomal RNA gene database project: improved data processing and web-based tools. Nucleic Acids Res 41:D590–D596

Rogato A, Amato A, Iudicone D, Chiurazzi M, Ferrante MI, d'Alcalà MR (2015) The diatom molecular toolkit to handle nitrogen uptake. Mar Genomics 24:95–108

Shaw PT (1992) Shelf circulation off the southeast coast of China. Rev Aquat Sci 6:1–28

Shih CY, Liu WC, Kuo TH, Chan YF and others (2021) Temporal variations in the expression of a diatom nitrate transporter gene in coastal waters off northern Taiwan: the roles of nitrate and bacteria. Cont Shelf Res 227: 104506

Shiomoto A, Sasaki K, Shimoda T, Matsumura S (1994) Kinetics of nitrate and ammonium uptake by the natural populations of marine phytoplankton in the surface water of the Oyashio region during spring and summer. J Oceanogr 50:515–529

Smith SL, Yamanaka Y, Pahlow M, Oschlies A (2009) Optimal uptake kinetics: physiological acclimation explains the pattern of nitrate uptake by phytoplankton in the ocean. Mar Ecol Prog Ser 384:1–12

Smith SR, Dupont CL, McCarthy JK, Broddrick JT and others (2019) Evolution and regulation of nitrogen flux through compartmentalized metabolic networks in a marine diatom. Nat Commun 10:4552

Song B, Ward BB (2007) Molecular cloning and characterization of high-affinity nitrate transporters in marine phytoplankton. J Phycol 43:542–552

Strickland JDH, Parsons TR (1972) A practical handbook of seawater analysis, 2nd edn. Bulletin 167. Fisheries Research Board of Canada, Ottawa

Suzuki S, Kataoka T, Watanabe T, Yamaguchi H, Kuwata A, Kawachi M (2019) Depth-dependent transcriptomic response of diatoms during spring bloom in the western subarctic Pacific Ocean. Sci Rep 9:14559

Syrett PJ, Flynn KJ, Molloy CJ, Dixon GK, Peplinska AM, Cresswell RC (1986) Effects of nitrogen deprivation on rates of uptake of nitrogenous compounds by the diatoms, *Phaeodactylum tricorutum* Bohlin. New Phytol 102: 39–44

Tsai SF, Wu LY, Chou WC, Chiang KP (2018) The dynamics of a dominant dinoflagellate, *Noctiluca scintillans*, in the subtropical coastal waters of the Matsu Archipelago. Mar Pollut Bull 127:553–558

Xu J, Gilbert PM, Liu H, Yin K, Yuan X, Chen M, Harrison PJ (2012) Nitrogen sources and rates of phytoplankton uptake in different regions of Hong Kong waters in summer. Estuaries Coasts 35:559–571

Zhang Y, Lin X, Shi X, Lin L, Luo H, Li L, Lin S (2019) Metatranscriptomic signatures associated with phytoplankton regime shift from diatom dominance to a dinoflagellate bloom. Front Microbiol 10:590

Editorial responsibility: Antonio Bode, A Coruña, Spain
Reviewed by: 3 anonymous referees

Submitted: February 4, 2023
Accepted: October 19, 2023
Proofs received from author(s): January 7, 2024